

WIND SHIELDING IN REFINING AND PETROCHEMICAL FACILITIES

BY

JEFFREY BARTO

THESIS

Submitted in partial fulfillment of the requirements
for the degree of Master of Science in Civil Engineering
in the Graduate College of the
University of Illinois at Urbana-Champaign, 2020

Urbana, Illinois

Adviser:

Professor Paolo Gardoni

ABSTRACT

The most influential climatic load affecting the structural design of gulf coast refining and petrochemical facilities is wind. Despite this fact, little has been done to customize wind design for these unique facilities. This paper proposes a probabilistic model to predict the magnitude of shielding that is provided by the vast network of pipe rack structures that encircle these densely arranged facilities. The probabilistic model is built from data obtained through a broad sampling of pipe rack configurations simulated with hurricane force winds using computational fluid dynamics (CFD). The CFD simulation approach is validated against published wind tunnel data that relate the proposed methodology to code recognized procedures (i.e. wind load reductions corroborated by wind tunnel testing). A reliability analysis is then carried out to re-calibrate the LRFD design equation to include the proposed shielding effects while maintaining the code specified level of reliability.

TABLE OF CONTENTS

CHAPTER 1: INTRODUCTION.....	1
CHAPTER 2: REVIEW OF WIND LOAD DEVELOPMENT.....	5
CHAPTER 3: CASE FOR CONSIDERING UPWIND SHIELDING IN REFINING AND PETROCHEMICAL FACILITIES.....	7
CHAPTER 4: FORMULATION OF THE PROPOSED PROBABILISTIC SHIELDING MODEL	10
CHAPTER 5: GENERATION OF SYNTHETIC DATA USING COMPUTATIONAL FLUID DYNAMICS (CFD).....	13
CHAPTER 6: SHIELDING MODEL CALIBRATION.....	20
CHAPTER 7: LRFD RE-CALIBRATION	23
CHAPTER 8: CONCLUSIONS	28
REFERENCES	30

CHAPTER 1: INTRODUCTION

The significant majority of refining and petrochemical facilities are located in coastal regions where hurricane force winds control the structural design. Yet the unique wind field characteristics of these facilities are not well understood. Design wind loads are generated through the use of governing design codes that have been developed primarily with data from the commercial building industry. Considerations for a general “roughness” of the upwind terrain are provided but no provisions for shielding from upwind structures on the design structure are included unless proven by wind tunnel testing. This is primarily due to the high level of variability of the typical cityscape. Obstructions are of varying heights, sizes, and spacing—all of which contribute to the uncertainty of shielding provided.

To date, the majority of research specific to wind shielding within refining and petrochemical facilities has focused on shielding between structural frames and equipment within the same open framed structure. Georgiou (1979) used a wind tunnel setup comprised of multiple frames of varying size, spacing, and solidity to study the shielding between adjacent frames. The findings showed appreciable shielding between frames dependent upon the properties of the frames. Georgiou et al. (1981) studied the effect of the wind angle of approach on the frame loads in the along-wind direction and found that the maximum load was incurred at an offset of approximately 15° for low porosity structures such as those found in refining and petrochemical facilities. Nadeem and Levitan (1997) further extended the work of Georgiou et al. by developing an empirical model which quantified wind loads on a set of frames orthogonal

to the wind direction as well as the along-wind frames. Their model was also capable of predicting the angle at which these maximum loads occur.

In addition to the structural frame shielding, Amoroso and Levitan (2009) recognized the impact that equipment, piping, and other auxiliary items can have on shielding within the typical open framed structure found in refinery and petrochemical facilities. Their approach abandoned the tedious consideration of each individual element and, instead, focused on a more generalized understanding of the wind load through measures of the porosity and length-to-width ratios of the structure. This generalized approach provided higher accuracy to wind tunnel data for low porosity structures collected by Qiang (1998) when compared against the tedious accounting of each individual element. These findings proved the method of superposition of each element in a theoretically isolated environment does not produce results that are well aligned with wind tunnel data for open framed structures.

The most commonly encountered element within refinery and petrochemical facilities is piping. In most cases, the piping is supported side-by-side within a structure, or rack. Therefore, it is not sufficient to only gain an understanding of the effects of a single pipe but, rather, it is important to understand the effects of multiple pipes arranged in-line. Liu et al. (2003) conducted extensive wind tunnel testing on arrangements of up to four pipes in-line. The results of the testing were used to produce force and lift coefficients for a plethora of arrangements with varying pipe sizes, spacing, and surface roughness as well as varying flow turbulence.

Aside from research focused on a particular design structure, Petersen et al. (1994) and Petersen (1990) sought to assess crude oil refineries based on the overall surface roughness and displacement heights (height at which wind turbulence is extremely high and the net load is negligible). These parameters can then be used to model toxic cloud dispersions which are of significant interest to facilities handling toxic substances. The results of the study indicated that both the surface roughness and displacement height specific to refineries are notably higher than those published in the US building codes for general urban and suburban settings.

While the typical city landscape is fraught with open areas such as parking lots, roads, and varying gaps between buildings, the landscape within refining and petrochemical facilities is significantly more dense and uniform. This unique environment presents the opportunity to quantify the effects of direct shielding provided by certain upwind obstructions that are consistent across the wind fetch of downwind design structures. An ideal obstruction exists with pipe rack structures that traverse these facilities in a linear, gridded manner creating a type of “wind fence” through-out.

This paper develops a probabilistic model to predict the amount of shielding pipe racks provide to downwind design structures. The model is formulated using the physical properties of pipe racks that contribute to the drag on wind flow. A dataset for developing the probabilistic model is built using Computational Fluid Dynamics (CFD) to simulate wind flow through a sample of pipe rack structures. The CFD simulations allow modeling and analyzing a multitude of arrangements efficiently. The CFD simulations are benchmarked against published wind tunnel data as solution verification and validation studies are imperative to understand the

accuracy and reliability of CFD models (Blocken 2014). Additionally, validating the CFD models against wind tunnel testing ties the results to a procedure recognized by ASCE/SEI-7 as a proven method for modifying wind pressures. Furthermore, the probabilistic shielding model is incorporated into the ASCE/SEI-7 wind pressure design equation and an LRFD load factor re-calibration is conducted. This process ensures the revised design with shielding produces the same level of reliability as the unshielded design.

The remaining of this paper is organized as follows. Section 2 reviews current industry practices. Section 3 outlines the case for considering shielding effects. Section 4 formulates the shielding model. Section 5 covers the generation of the dataset using the CFD simulations. Section 6 calibrates the shielding model. Section 7 presents the LRFD re-calibration. Finally, Section 8 presents conclusions, implementation limitations, and recommendations for future work.

CHAPTER 2: REVIEW OF WIND LOAD DEVELOPMENT

Calculating wind load on a structure begins with determining the appropriate wind pressure based on wind speed and a host of environmental factors such as upwind roughness, topography, and height above grade. The calculated wind pressure is then converted into a wind load through the physical characteristics of the design structure, such as structural stiffness, and the effects of the shape and aspect ratio on the wind forces.

2.1. Code-based Procedures

The code basis for wind load development in the United States is ASCE/SEI-7, Minimum Design Loads and Associated Criteria for Buildings and Other Structures (ASCE 2016). As the name implies, however, it was developed primarily with typically commercial buildings in mind. Design wind pressures are calculated per Eqn 26.10-1 (ASCE 2016). Primary inputs in this equation include the environmental components that have an impact on the wind flow field. This includes the velocity pressure exposure coefficient that considers the general “roughness” of the ground surface. This roughness measure captures the drag effect of surface obstructions of average size on the overall boundary wind layer, which most often extends vertically a thousand feet or more above the earth’s surface. This effect develops over long ranges of up to one-half mile of persistent surface roughness. Thus, the consideration of these long range drag effects are important to estimating the wind pressure that arrives at a particular design structure. However, it does not address the localized effects a particular upwind structure can have on the design structure. Such an effect is currently only allowed by code when corroborated through wind tunnel testing.

2.2. Current Refining and Petrochemical Industry Practice

The only design factor currently customized for structures in refining and petrochemical facilities is the force coefficient, C_f . ASCE has released guidance on this factor through the ASCE Wind Guide for Petrochemical and Other Industrial Facilities (ASCE 2011). The guidance allows for C_f to be assessed on a structure-wide basis considering shielding between structural frames and equipment rather than the summation of wind loads from each individual component irrespective of surrounding elements. Although this guidance allows for shielding within a structure, there is no accommodation made for the effects of shielding between separate structures. The commentary to ASCE/SEI-7 identifies the lack of “reliable analytical procedures” as the primary reason for excluding consideration of upwind shielding in the code’s prescriptive design procedures.

CHAPTER 3: CASE FOR CONSIDERING UPWIND SHIELDING IN REFINING AND PETROCHEMICAL FACILITIES

The unique density and uniformity of refining and petrochemical facilities (Fig. 1) presents an environment that mitigates the shielding uncertainties that plague typical urban and suburban landscapes.



Fig. 1: Example of a refinery

The main processing areas of refining and petrochemical plants are comprised of “units” arranged in a grid pattern. These units are joined by an interconnected maze of open frame type structures called pipe racks (Fig. 2) which ferry pipes and cables throughout the entire plant. It is also common to support a particular type of equipment, referred to as “air coolers”, on top of pipe racks.



Fig. 2: Example of Pipe Rack

Pipe rack structures serve a critical function in the plant by connecting equipment, vessels, and tanks throughout each unit and among many other units within the plant. This means that pipe racks are layered with elements that serve multiple units. For this reason, pipe racks enjoy extensive longevity as it is extremely difficult and expensive to remove a pipe rack and, thus, is extraordinarily rare. Therefore, by extension, shielding considerations for pipe racks can be considered permanent for the vast majority of design cases. If a pipe rack is being removed, it is almost certain the surrounding equipment and structures—which were affected by shielding from the pipe rack—are being removed as well.

The ubiquity and uniformity of pipe rack structures throughout refining and petrochemical facilities can be thought of as a grid of “wind fences” (Fig. 3). Also, the vast majority of racks do not terminate but, rather, tie into perpendicular racks. This avoids “open areas” which can have localized wind effects.

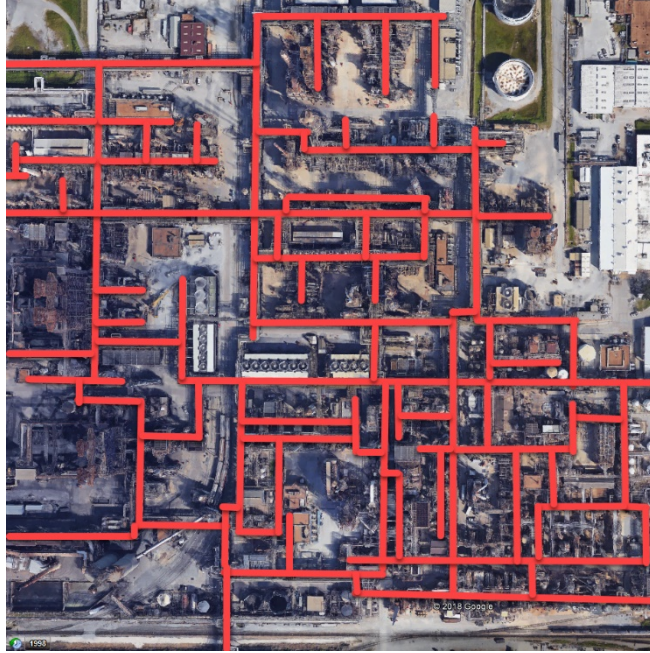


Fig. 3: Traced Pipe Rack Arrangement in a Refinery

The density of pipe racks shown in Fig. 3 can be compared in a holistic sense to the considerations of shielding among different frames within the same structure already allowed in the ASCE published guidance—simply on a larger scale. For the reasons outlined in this section, we believe pipe racks present a unique opportunity to predictably consider upwind shielding within refining and petrochemical facilities.

CHAPTER 4: FORMULATION OF THE PROPOSED PROBABILISTIC SHIELDING MODEL

To introduce upwind shielding considerations into the code-based framework, we need to develop a predictive model by which a designer can input a set of parameters to quantify the shielding effect rather than explicitly testing each design iteration. We use CFD simulations over a wide range of potential variables to validate our approach and provide the data required to calibrate the proposed model.

4.1. Model Formulation

With the understanding that drag, and thus shielding, is dependent upon the physical attributes of a structure, we develop a model that captures the key geometric characteristics \mathbf{x} of a pipe rack. Following Gardoni et al. (2002), we introduce “explanatory functions” to capture such geometric characteristics through a meaningful functional form. To aide the implementation as a design factor in the code equations, the explanatory functions are taken as dimensionless through the use of a baseline quantity. Each explanatory function is then multiplied by an unknown model parameter that quantifies its impact on the shielding effect. Lastly, a model error is included to capture the model inexactness for inclusion in the reliability analysis. Bringing all these model components together, we then have the shielding model of the form (Gardoni et al. 2002)

$$S(\mathbf{x}, \Theta) = \gamma(\mathbf{x}, \theta) + \sigma\varepsilon \quad (1)$$

where $S(\mathbf{x}, \Theta)$ is the natural logarithm of the ratio of shielded, squared velocity to unshielded, squared velocity, $\gamma(\mathbf{x}, \theta)$ is defined by the “explanatory functions”, and $\sigma\varepsilon$ is the

model error. The unknown parameters in the model are $\Theta = (\boldsymbol{\theta}, \sigma)$. The velocity terms are squared to align with the ASCE/SEI-7 code equation for wind pressure which is predicated on the square of the velocity to produce the force representation of interest, i.e., the wind pressure. The logarithmic variance-stabilizing transformation is used to approximately satisfy the homoskedasticity assumption (i.e., σ is constant over the range of \boldsymbol{x}), the normality assumption (i.e., ε follows a standard Normal distribution), and the additivity assumption of the model error.

The term $\gamma(\boldsymbol{x}, \boldsymbol{\theta})$ is written as

$$\gamma(\boldsymbol{x}, \boldsymbol{\theta}) = \sum_{i=1}^p \theta_i h_i(\boldsymbol{x}) \quad (2)$$

where p is the number of explanatory functions, $h_i(\boldsymbol{x})$. The choice of the explanatory functions is based on industry experience reflecting the common geometric attributes of pipe racks. Table 1 lists the candidate explanatory functions considered to construct the proposed probabilistic model.

Table 1: Explanatory Functions

Physical Variables, x	Explanatory Functions, $h_i(x)$ ¹	Baseline Values	Sample Range
Design Structure Relative Height ³	$h_1=[r_i - r_0(1.05)]^2 / R_b$	$R_b=[r_0 - r_0(1.05)]^2$	r_i : 15ft – 69ft
Downstream Distance	$h_2=l_i / L_b$	$L_b=50\text{ft}$	l_i : 50ft - 150ft
Width of Rack	$h_3=w_i / W_b$	$W_b=20\text{ft}$	w_i : 10ft - 30ft
Height to Lowest Rack Level	$h_4=c_i / C_b$	$C_b=15\text{ft}$	c_i : 12ft - 18ft
Air Coolers	$h_5=Y/N$	N/A	Y=1; N=0
Cumulative Obstruction Windward Height ²	$h_6=o_i / O_b$	$O_b=5.6\text{ft}$	o_i : 5.6ft - 18.5ft
Centroid of Effective Windward Height ²	$h_7=a_i / A_b$	$A_b=20.9\text{ft}$	a_i : 17.9ft - 48.8ft

¹ Baseline values used in denominators to produce dimensionless results.

² Obstruction height and centroid measurements include structural steel, piping, cable tray, and air coolers (certain scenarios).

³ r_0 taken as the height of the shielding pipe rack

CHAPTER 5: GENERATION OF SYNTHETIC DATA USING COMPUTATIONAL FLUID DYNAMICS (CFD)

The CFD process discretizes the fluid (air in this case) domain and surfaces within the model and relies upon extensive numerical integration techniques to solve for physical quantities of interest. These techniques are complex and the computational demands for solving large models can be significant. Recent advancements in computing have made it possible to run fairly complex models on a personal computer in a reasonable timeframe. As such, CFD tools have become a boon to study a wide variety of wind flow configurations without having to build physical, scale-model representations of each for wind tunnel testing.

Several well-developed software options exist in the marketplace for CFD simulations. Autodesk CFD 2019 is chosen for this research due to its widespread availability with a large user base, proven technical support, and interoperability with modeling software. Within the CFD simulation solver, the K-Omega Shear Stress Transport (SST) turbulence model (Menter 1993) is used. This turbulence model is a good fit for this application as it is a hybrid model combining the near-wall strengths of the k-Omega turbulence model with the stabilization of the k-Epsilon turbulence model for regions further away from surfaces (Autodesk 2013).

Meshing best practices including wall layers and dense mesh blending in regions of high turbulent kinetic energy are applied and heavily scrutinized throughout to attain the most efficient balance between precision and computing efficiency. Although not explicitly detailed in this paper, the accuracy of these methods can be seen through the benchmark validation efforts to

recreate wind tunnel results as outlined in Section 5.2. Successful meshing practices from validation models are carried over to the pipe rack models.

5.1. CFD Modelling Techniques and Considerations

Typical buildings are composed of an assemblage of generally large, bluff surfaces, which are well understood in terms of drag characteristics. Open frame structures such as pipe racks, however, contain smaller length scales and shapes that complicate the wind field effects significantly. Therefore, a level of accuracy must be attained at the individual component level that can then be extended to the holistic pipe rack structure.

The small length scales in pipe racks lead to drag sensitivities to a non-dimensional flow parameter known as the Reynolds number (ASCE 2011). The Reynolds number relates the inertial forces in a flow field to the viscous forces in the flow field as shown in Eq. 3, where U is the flow velocity, D is a characteristic dimension for the structure or element, and ν is the kinematic viscosity.

$$Re = \frac{U \times D}{\nu} \quad (3)$$

In the range of flow that is present in hurricane force wind design, many structural forms will not exhibit notable sensitivity of the force coefficient to the Reynolds number, with the exception of curved surfaces (ASCE 2011). Within the range of sizes of curved surfaces, the sensitivity changes significantly. For instance, cylindrical surfaces such as vessels and drums typically do not exhibit sensitivity to the Reynolds number. Yet within the same wind field, handrail and smaller piping can exhibit significant sensitivities (ASCE 2011). These sensitivities

are best captured in CFD simulations through meticulous mesh development and specialty turbulence models adept at “reverse curvature” scenarios. These tradeoffs are discussed further in Section 5.2. Fortunately, bluff objects such as structural steel, cable trays, and air coolers do not share these same sensitivities as the well-defined corners provide consistency in shear layer separation.

This paper considers two dimensional (2D) CFD simulations. Wind tunnel testing of open framed structures has shown that the angle of incidence that produces the largest load effect is skewed from the orthogonal direction (Amoroso and Levitan 2009). As a result, an increased measure of drag would be realized with 3D CFD models. However, the computing power required would necessitate the use of supercomputing. Since the maximum load incurred is related to the amount of drag, forming a basis for the shielding model with 2D analyses (which do not consider a skewed wind scenario) yields conservative results for the amount of real-world drag.

5.2. Benchmark Validation and Error

With the design code acceptance of wind tunnel testing as a means of more accurately estimating wind loads, we validate the CFD analyses using available wind tunnel testing data for similar scenarios.

Wind drag and shielding on multiple frames aligned in the direction of the applied wind was studied through wind tunnel testing conducted by Georgiou et al. (1981). As noted previously, CFD simulations comprised of bluff surfaces have been successful in reproducing results that are well aligned with wind tunnel test data. With regards to the Georgiou study, the

CFD simulation was able to produce drag coefficients with less than 0.25% variation from the published results.

Cylindrical objects such as piping, however, face more variability. As previously discussed, the Reynolds Number sensitivities of these surfaces make it difficult to accurately predict the drag characteristics. This is true in wind tunnel testing such as Liu et al. (2003) and Gu et al. (1993), as well as CFD simulation. These uncertainties are further complicated by the innumerable combinations of pipe spacing and sizing that are found in real world applications.

Despite the significant headwinds to assess the accuracy of flow around pipes, there is still a need to better understand and quantify this effect. To this end, we pursued extensive, detailed CFD simulations to reproduce the published wind tunnel data collected. Reverse-curvature type turbulence models are found to be the most accurate at capturing cylindrical surface sensitivities. For a single pipe, these models can be quite accurate at replicating wind tunnel results. However, the more pipes involved and the multitude of size and spacing combinations hampered our ability to precisely quantify error against wind tunnel data that itself varied significantly from study to study. Furthermore, reverse-curvature turbulence models are specifically attuned to the sensitivities of curved surfaces and do not extend well to the holistic pipe rack structure. Fortunately, the parameter of interest—the downwind pressure—has been shown to be less reliant upon the minutia of the wake structures coming off the curved piping surfaces. CFD benchmarking models reflecting up to 30-40% variations in drag coefficients have only shown variations within approximately 5% of downwind pressure using the chosen k - Ω SST turbulence model. When compared against other available turbulence models, the

downwind pressures produced under the k-Omega SST turbulence models are consistently higher, which implies some conservatism.

Although isolated flow regimes around a pipe require significantly more robust modeling approaches, the confluence of these flow regimes within the larger context of a pipe rack structure featuring bluff surfaces and the multiple adjacent pipes placed in close succession serves to increase turbulence that in turn mutes these unique flow effects. The effects of higher turbulence intensity have been shown to decrease the Reynolds Number sensitivities (Liu et al. 2003).

The wind flow through an open frame structure such as a pipe rack can be holistically compared to that of porous wind fences. Benchmark validation models using the k-Omega SST turbulence model exhibit excellent alignment with wind tunnel results. Specifically, the reattachment length parameter of these wind tunnel studies was chosen as a good proxy for the downwind flow measurements. This parameter quantifies the downwind distance it takes for the flow to “reattach” after the reverse wake structure created in the fluctuating pressures behind the wind fence. The variation between the CFD simulation and published wind tunnel data (Dong et al. 2007) was under 1%.

A look back at the various benchmarking validation studies undertaken reveals excellent alignment with wind tunnel testing for bluff body frames and downstream reattachment. The only notable variation exists in the context of curved surfaces such as piping. When compared against published drag coefficients in five wind tunnel arrangements of varying numbers of

pipes, size, and spacing (Liu et al. 2003), the drag coefficients measured in the CFD simulations are an average of 25% lower than the wind tunnel results. A lower drag coefficient is intuitively correlated to a higher downwind velocity. Thus, the results observed indicate that the CFD simulations tend to give conservative results for downwind shielding effects.

The combination of low error related to bluff surfaces and downstream reattachment, consistently higher downwind pressures in CFD for curved surfaces (thus, more conservative for the purposes of measuring shielding), and the lack of wind tunnel testing of an actual pipe rack scale model justify using the downwind pressure results from the CFD simulations without any modification. This approach is expected to yield consistently conservative results. Any attempt to provide further precision in this regard would require a large number of additional wind tunnel tests specific to pipe rack structures.

5.3. Data Generation

In the context of the CFD simulations, shielding is quantified by averaging the wind (fluid) velocity downwind of the shielding pipe rack over the design structure relative height. An inlet wind velocity of 130 mph (209.2 km/h) is used to represent typical Gulf Coast locations where most oil and gas facilities are located in the United States. Considering the 130 mph wind speed puts the flow into the supercritical Reynolds Number range, the results can be reasonably extended to higher wind speeds.

A sampling of shielding pipe rack arrangements, downstream distance to the design structure, and relative height of the design structure are selected based on industry standards to

reflect the conditions most commonly encountered in refining and petrochemical facilities. In total, forty-six different pipe rack scenarios are simulated.

CHAPTER 6: SHIELDING MODEL CALIBRATION

A linear regression is used to estimate the unknown parameters Θ (Box and Tiao 1992). A step-wise deletion process (Gardoni et al. 2002) is conducted to simplify the model by removing less prominent terms which do not have a significant impact on model accuracy. Fig. 4 show the process as explanatory functions are removed based on the values of the coefficient of variation of the model parameters, and the model accuracy is assessed. The process is terminated at Step 4 since removal of h_7 would lead to a significant loss of accuracy (i.e. a significant increase in σ). Step 5 experiences an increase in σ of approximately 18%.

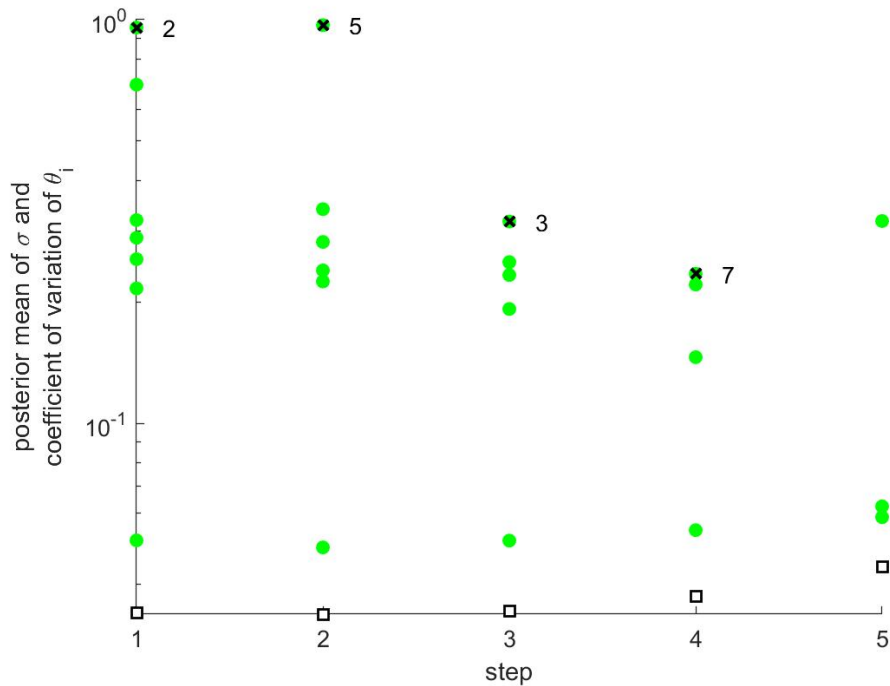


Fig. 4: Step-wise deletion

Through this procedure, the seven initial explanatory functions are reduced to four as shown in Eqn. 4 and with the parameters shown in Table 2.

$$S(\mathbf{x}, \Theta) = \theta_1 h_1(\mathbf{x}) + \theta_4 h_4(\mathbf{x}) + \theta_6 h_6(\mathbf{x}) + \theta_7 h_7(\mathbf{x}) + \sigma \varepsilon \quad (4)$$

Fig. 5 shows the comparison of the proposed shielding model against the raw CFD simulation data along with (+/-) 1 standard deviation lines.

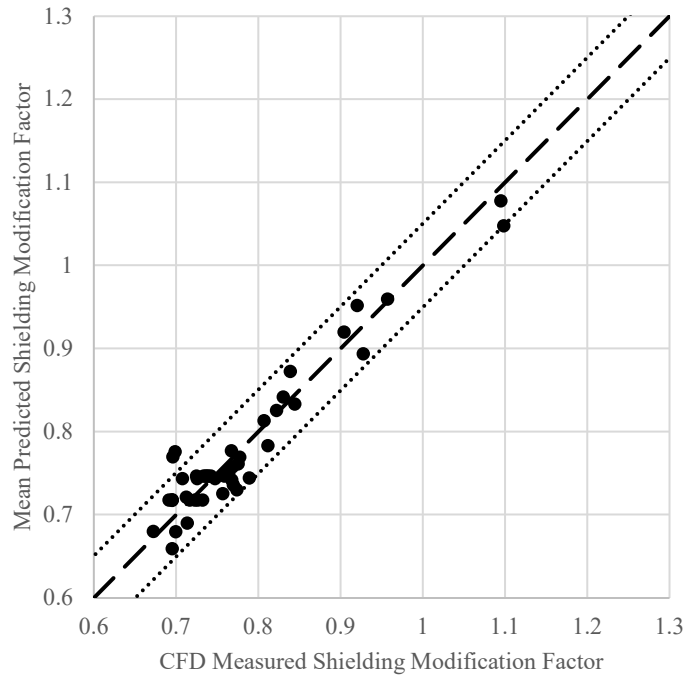


Fig. 5: Comparison of the estimates based on the proposed shielding model and raw CFD data

Under certain circumstances, the shielding factor produces an increase in wind pressure. This is an indication of the flexibility of the model to uncover unique scenarios such as a design structure with a low relative height that is more exposed to the tunneling effect that occurs

underneath the bottom level of the pipe rack. In this scenario, the design structure does not have the height to take advantage of the shielded flows behind the more obstructed portions of the pipe rack and, therefore, sees the appropriate increase in design wind pressure.

CHAPTER 7: LRFD RE-CALIBRATION

This section carries out a reliability analysis to re-calibrate the current LRFD wind load factor in ASCE/SEI 7-16 with the inclusion of the proposed shielding modification factor. The re-calibration is done considering the code-specified target reliabilities stated in Table 1.3-1 of ASCE/SEI 7-16. All pertinent load and resistance uncertainties—including those associated with the shielding model—are included. The re-calibration produces a modified LRFD wind load factor which considers the shielding modification factor and maintains a consistent level of reliability with the current unshielded approach.

7.1. Development of Limit State Function

A simple, braced design structure is chosen for the reliability analysis as shown in Fig 6. The structure is arranged such that the effective area is assumed to all contribute to the lateral wind force being transmitted into a tension brace at a 45 deg angle. The tension member is then assumed to fail in tension yielding for the purposes of conducting a component reliability analysis.

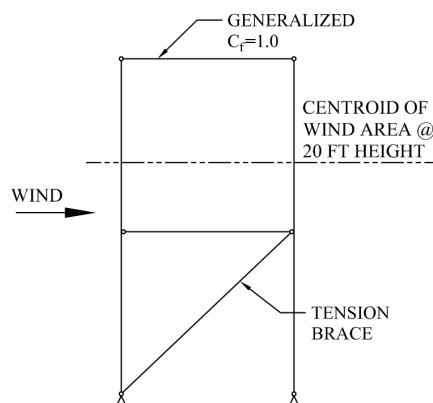


Fig. 6: Design Structure for Component Reliability Analysis

The code design equations without shielding and only accounting for wind loads are

$$0.9R = 1.0W_n \quad (5)$$

$$R = A_s F_y \quad (6)$$

$$W_n = 1.414 \times (0.00256K_z K_{zt} K_d K_e V^2) \times C_f G A \quad (7)$$

The 1.414 multiplier comes from the 45 degree inclination of the tension member. The remaining deterministic values used to calculate the design value of area of steel required, A_s , can be found in Table 2.

Table 2: Design Equation Deterministic Values

Variable	Value
F_y	36 ksi
K_z	0.9 (Exp. Cat. C at 20ft)
K_{zt}	1
K_d	0.85
K_e	1.0 (sea level)
V	130 mph (Baton Rouge, LA)
C_f	1.0 (generalized)
G	0.85 (rigid)
A	200 ft ²

The limit state equation for an unshielded design is of the form

$$g(R, K_z, V, G) = R - 1.414 \times 0.00256K_z K_{zt} K_d K_e V^2 \times C_f G A \quad (8)$$

where the distributions of the random variables are provided in Table 3.

Table 3: Limit State Equation Probabilistic Distributions

Variable	Description	Distribution	Mean/ Nominal	C.O.V.	References
$R=A_s*F_y$	Tension limit state resistance	Lognormal	1.05	0.11	(ANSI A58 1980)
K_z	Velocity pressure exposure coefficient	Normal	0.93	0.143	Exp. Cat. C @ 20ft (Ellingwood and Tekie 1999)
V	Design wind speed (mph)	Gumbel	0.503	0.297	Baton Rouge, LA (Vickery et al., 2000 and Amoroso, 2007)
G	Gust effect factor	Normal	0.965	0.098	(Ellingwood and Tekie 1999)

Including the shielding model produces a new form of the W_n design equation and the limit state equation as follows

$$W_n = 1.414 \times (0.00256K_zK_{zt}K_dK_eV^2) \times C_fGA \times [\theta_1h_1(\mathbf{x}) + \theta_4h_4(\mathbf{x}) + \theta_6h_6(\mathbf{x}) + \theta_7h_7(\mathbf{x})] \quad (9)$$

$$g(R, K_z, V, G, \theta_1, \theta_4, \theta_6, \theta_7, \sigma) = R - 1.414 \times 0.00256K_zK_{zt}K_dK_eV^2 \times C_fGA \times [\theta_1h_1(\mathbf{x}) + \theta_4h_4(\mathbf{x}) + \theta_6h_6(\mathbf{x}) + \theta_7h_7(\mathbf{x}) + \sigma\varepsilon] \quad (10)$$

where probabilistic data for the shielding parameters, θ_i , and model error, σ , are provided in Table 4.

Table 4: Optimized Shielding Model Parameters

Parameter	Mean	Standard Deviation	Correlation Coefficient				
			θ_1	θ_4	θ_6	θ_7	σ
θ_1	0.0015	0.0001	1.000				
θ_4	-0.7236	0.1055	0.1518	1.000			
θ_6	-0.3432	0.0757	0.1326	0.9812	1.000		
θ_7	0.7732	0.1814	-0.1540	-0.9928	-0.9968	1.000	
σ	0.0373	0.0040	-0.0144	-0.0551	-0.0634	0.0601	1.000

Within refining and petrochemical facilities, the vast majority of construction above grade is done with structural steel. Accordingly, probabilistic distributions for the appropriate structural steel limit state is pulled from well-established, code-cited research (ANSI A58 1980) and shown in Table 3.

7.2. Calibration to Target Reliability

An LRFD load factor re-calibration is carried out to align the design reliability including shielding to the target reliability index of 3.25 per Table 1.3-1 reflecting risk Category III (common for refining and petrochemical facilities which contain hazardous materials) and corresponding to a “failure that is not sudden and does not lead to widespread progression of damage” (ASCE 2016).

The shielding model estimates for the forty-six CFD pipe rack configurations are used for the re-calibration. The shielding model estimates an average factor of 0.78 with a coefficient of variation of 0.115. Per Eq. C2.3-1 from ASCE/SEI 7-16, this produces a re-calibrated LRFD load factor of 1.02. On average, the shielding model results in an unfactored wind load reduction of 22%. When factored to include the relevant uncertainties, this average drops to 20% which still represents a significant optimization over current methods. One should note this average

reduction includes instances over the range of the simulation scenarios where the model actually results in an increase in wind pressure.

This code provided re-calibration approach is further verified using a single scenario corresponding to the pipe rack configuration with baseline parameter values. This configuration is adjudged to be the most common pipe rack configuration encountered in facilities based on the author's experience. A reliability analysis utilizing the first-order reliability method (FORM) is first run without shielding and considering all load and resistance uncertainties previously discussed. The shielding model probabilistic variables and the proposed LRFD load factor of 1.02 are then included and the same analysis is rerun. The result produces a reliability index approximately 1% higher than the unshielded analysis. The slight conservatism is due to rounding up of the re-calibrated LRFD load factor. This analysis further confirms the proposed method maintains a consistent level of reliability with current code-based methods.

CHAPTER 8: CONCLUSIONS

The vast majority of the built environment contains such variability in the size and spacing of obstructions that shielding considerations are only allowed by design codes when validated through wind tunnel testing. Within refining and petrochemical facilities, however, the uniformity and ubiquity of pipe racks presents a localized environment wherein shielding effects become more predictable. Taking advantage of this opportunity, a probabilistic model is developed to relate the magnitude of wind shielding to the geometric characteristics of the shielding pipe rack and associated design structure.

Across the forty-six scenarios simulated in CFD and leveraged to develop the probabilistic shielding model, the shielding model predicts an average reduction of 22% from the code calculated wind pressure. The ability of the model to capture both reductions and increases in specific arrangements is a key strength of the multi-parameter approach.

It is important to note the limitations to implementations of the shielding model. Unique scenarios that lie outside the range of the explanatory functions could produce results that have not been verified by the model. Additionally, the distance between the shielding structure and downwind structure in the scenarios considered ranges from a ratio of one to four times the height of the shielding structure. Conditions outside this range could also produce unverified results.

Considering the study used 2D CFD modelling, we must be cognizant of the 3D impacts in a real-world implementation. We must ensure there is consistency and breadth of the shielding pipe rack to maintain the conditions necessary for shielding. To meet this need, we recommend utilizing a 45-degree influence line in each direction from the design structure. Within the area bounded by the influence lines, the most unconservative pipe rack arrangement in terms of wind pressure reductions should be used. This ensures that adjacent inconsistencies do not adversely affect the model prediction.

Although the focus of this study has been the influences of a single pipe rack shielding on downwind structures, the multi-layered nature of pipe racks throughout refining and petrochemical facilities lends itself well to an extension of this study to examine the compounding impacts of several pipe racks across a particular upwind fetch.

REFERENCES

- Amoroso, S. (2007). Wind Loads for Petrochemical Structures. *LSU Doctoral Dissertation*.
- Amoroso, S., Levitan, M. (2009). Wind Loads for High-Solidity Open Frame Structures. *11th Americas Conference on Wind Engineering, San Juan, Puerto Rico, June 22-26*.
- ANSI A58, Ellingwood, B., Galambos, T., MacGrigor, J., Cornell, C. (1980). Development of a Probability Based Load Criterion for American National Standard A58. *Building Code Requirements for Minimum Design Loads in Buildings and Other Structures*.
- ASCE (2011) Wind Loads for Petrochemical and Other Industrial Facilities. *Task Committee on Wind Induced Forces of the Petrochemical Committee of the Energy Division, American Society of Civil Engineers, New York*.
- ASCE (2016) Minimum Design Loads for Buildings and Other Structures. *ASCE Standard SEI/ASCE 7-16, American Society of Civil Engineers, Reston, VA*.
- Autodesk CFD Support Hangout #5 (2014). <https://www.youtube.com/watch?v=Yf2iVABc8cg>.
- Blocken, B. (2014). 50 years of Computational Wind Engineering: Past, present and future. *Journal of Wind Engineering and Industrial Aerodynamics*, **129**, 69-102.
- Box, G. E. P., and Tiao, G. C. (1992). *Bayesian inference in statistical analysis*, Addison–Wesley, Reading, Mass.
- Dong, Z., Luo, W., Qian, G., Wang, H. (2007). A wind tunnel simulation of the mean velocity fields behind upright porous fences. *Agricultural and Forest Meteorology*, **146**, 82-93.
- Ellingwood, B., Tekie, P. B. (1999). Wind Load Statistics for Probability-Based Structural Design. *Journal of Structural Engineering*, **125(4)**, 453-463.
- Gardoni, P., Der Kiureghian, A., Mosalam, K. (2002). Probabilistic Capacity Models and Fragility Estimates for Reinforced Concrete Columns based on Experimental Observations. *Journal of Engineering Mechanics*, **128(10)**, 1024-1038.
- Georgiou, P.N. (1979) A Study of the Wind Loads on Building Frames, *Masters Thesis, University of Western Ontario, Canada*.
- Georgiou, P. N., Vickery, B. J., Church, R. (1981). Wind loading on Open Framed Structures. *3rd Canadian Workshop on Wind Engineering, Vancouver, April 1981, and Toronto, May 1981*.

- Gu, Z. F., Sun, T. F., He, D. X., Zhang, L. L. (1993). Two supercritical cylinders in high-turbulence flow at supercritical Reynolds number. *Journal of Wind Engineering and Industrial Aerodynamics*, **49**, 379-388.
- Liu, X., Levitan, M., Nikitopoulos, D. (2008). Wind tunnel tests for mean drag and lift coefficients on multiple circular cylinders arranged in-line. *Journal of Wind Engineering and Industrial Aerodynamics*, **96**, 831-839.
- Menter, F. R. (1993). Zonal Two Equation $k-\omega$ Turbulence Models for Aerodynamic Flows. *AIAA Paper* **93-2906**.
- Murphy, C., Gardoni, P., Harris, C.E., (2011). Classification and moral evaluation of uncertainties in engineering modeling. *Science and Engineering Ethics*, **17** (3), 553-570.
- Nadeem, A., Levitan, M. (1997). A refined method for calculating wind load combinations on open-framed structures. *Journal of Wind Engineering and Industrial Aerodynamics*, **72**, 445-453.
- Qiang, L. (1998) Wind Tunnel Tests for Wind Loads on Open Frame Petrochemical Structures, *Masters Thesis, Louisiana State University, Baton Rouge, LA, 204p*.
- Petersen, R. (1990). Effect of homogeneous and heterogeneous surface roughness on heavier-than-air gas dispersion. *Journal of Wind Engineering and Industrial Aerodynamics*, **36** (1), 643-652.
- Petersen, R., Parce, D. (1994). Development and Testing of Methods for Estimating Surface Roughness Length at Refineries. *Cernak Peterka Petersen, Inc. Project 92-0890, prepared for American Petroleum Institute*.
- Vickery, P. J., Skerlj, P. F., and Twisdale, L. A. (2000). Simulation of hurricane risk in the U.S. using empirical track model. *Journal of structural eng.*, **126** (10), 1222 – 1237.